

Spatially inhomogeneous time-periodic propagating waves in anharmonic systems

Thierry Cretegny*

Laboratoire de Physique de l'École Normale Supérieure de Lyon, CNRS URA 1325, 69364-Lyon Cedex 07, France

Serge Aubry†

Laboratoire Léon Brillouin (CEA-CNRS), CE Saclay, 91191-Gif-sur-Yvette Cedex, France

(Received 18 February 1997)

Strongly anharmonic and translationally invariant systems in arbitrary dimensions, exhibit a class of time periodic and stable solutions carrying an energy flow as well as the standard plane waves which are special cases. In general, the spatial distribution of these energy flows is very inhomogeneous and form arbitrarily complex networks of channels and vortices. These solutions are constructed from arbitrary, finite, or infinite clusters of breathers (multibreathers) with twisted phases. Examples of these solutions are numerically calculated in several one and two-dimensional nonlinear models. [S0163-1829(97)50718-1]

It is well known that the energy flow carried by a plane wave in translationally invariant and harmonic systems, is spatially uniform. The aim of this paper is to show that in strongly anharmonic systems and despite that the translational invariance of the system is preserved, the propagation of a high density of energy at a fixed frequency can become nonuniform with drastically inhomogeneous energy flows.

These results are obtained as an application of recent developments of the theory of breathers based on the concept of anticontinuity.⁵ Breathers are spatially localized time periodic modes (breathers) which show up spontaneously in the numerical simulations of a large number of nonlinear models.^{1,2} Their existence as exact and stable solutions have been subsequently proven in Ref. 3 in finite or infinite time reversible arrays of coupled anharmonic oscillators in arbitrary dimensions, provided the coupling between particles be not too large, that is in the regime of strong anharmonicity. In addition to the existence of single breather solutions, the same theory yields the existence of proof of infinitely many other multibreather solutions among which an infinite and large subset has been proven to be linearly stable.⁵

At the anticontinuous limit, the system is an array of decoupled anharmonic oscillators and each oscillator is either periodically oscillating or is at rest. The time periodic and time reversible solutions with period t_b correspond to an arbitrary distribution of oscillators at rest and of moving oscillators at the given period and with phase 0 or π . Any of these solutions can be continued at finite coupling up to an upper bound which is proven to be nonzero³ and independent on the choice of the moving oscillators. The continued solution which involves initially only one moving oscillator, is just a single breather. The other solutions are multibreathers and we say that the breathers are located at the site where the oscillators were initially moving with a phase 0 or π . When the number of breathers is one or is finite, the corresponding solution decays exponentially at infinity. When the number of breathers is infinite, they could be spatially ordered, then appearing as spatially periodic waves, but can also have any spatial chaotic distribution or any other special kind of order. The initial condition of time reversibility (i.e., all the veloci-

ties are zero at the initial time) implies that these multibreather solutions cannot carry any energy current in average.

Actually, the time reversibility condition can be dropped and it is proven that there exists multibreather solutions that involve a ‘‘phase torsion’’ between the breathers and thus which carry an energy flow.⁵ An effective action $\Phi(\{\alpha_i\})$ can be defined as a 2π periodic function of the phase α_i of each breather at site i (if any) invariant under any global rotation of the phases. An exact solution is associated with each extremum of $\Phi(\{\alpha_i\})$. In time reversible systems, the configurations with $\alpha_i=0$ or π are extrema and are the time reversible multibreather solutions. This function $\Phi(\{\alpha_i\})$ is analogous to the Hamiltonian of an XY model which couples the phases of the breathers. Thus we will not be surprised to find extrema for which the breather phases are twisted by boundary conditions (‘‘phasons’’) or vortexlike solutions in two-dimensional models. In the simplest case with a breather at each site and a uniform twist, the standard plane waves propagating energy (but in an anharmonic system), will be recovered.

The Hamiltonians of the systems we choose as examples, for studying these solutions, have the form

$$\mathcal{H} = \sum_n \frac{\dot{u}_n^2}{2} + V(u_n) + \frac{C}{2} \sum_{\langle n,m \rangle} (u_n - u_m)^2, \quad (1)$$

where $V(u)$ is an anharmonic potential which can be ‘‘hard’’ [the phonon frequency increases with the amplitude, e.g., the quartic potential $V(u) = u^2/2 + u^4/4$] or the reverse called ‘‘soft’’ [e.g., the Morse potential $V(u) = \frac{1}{2}(1 - e^{-u})^2$]. C is the coupling constant between the nearest-neighboring sites n and m of the lattice. The dynamical equation associated with Eq. (1) is

$$\ddot{u}_i + V'(u_i) - C\Delta u_i = 0, \quad (2)$$

where $\Delta u_i = \sum_{j:\langle i,j \rangle} (u_j - u_i)$ is the discrete Laplacian and periodic boundary conditions are imposed.

Systematic and highly accurate numerical methods for calculating any time reversible breather or multibreather so-

lution continuing the trivial solution existing at $C=0$ have been developed in Ref. 4. We briefly describe how they are adapted for calculating the non-time-reversible solutions presented here.

Defining the nonlinear Poincaré map $X(t_b) = (\{u_i(t_b), \dot{u}_i(t_b)\}) = T_b[X(0)]$ by integration of Eq. (2) with the initial conditions $X(0) = (\{u_i(0), \dot{u}_i(0)\})$, the fixed points of this map T_b determine the initial conditions of the time periodic solutions of Eq. (2). We also define the linear tangent map $L_b(X)$ of $T_b(X)$ from the linearized Eq. (2),

$$\ddot{\epsilon}_i + V''(u_i)\epsilon_i - C\Delta\epsilon_i = 0, \quad (3)$$

which yields that $\{\epsilon_i(t)\}$ depends linearly on its initial conditions and determines $(\{\epsilon_i(t_b)\}, \{\dot{\epsilon}_i(t_b)\}) = L_b(\{\epsilon_i(0)\}, \{\dot{\epsilon}_i(0)\})$.

Starting from a trivial solution at $C=0$, parameter C is incremented by small steps. Each obtained solution at value C is taken as the trying solution at $C + \delta C$ of a modified Newton process for finding these fixed points based on three algorithms used sequentially in an appropriate fashion:

Algorithm 1: The standard Newton method consists in the recursive application of the operator $\{X' = X - [L_b(X) - 1]^{-1}[T_b(X) - X]\}$ to an initial trying solution chosen close enough to the real solution. This method cannot be applied for the free system in that way because $\{\epsilon_i(t) = \dot{u}_i(t)\}$ is a time periodic solution of Eq. (3) which implies that $[L_b(X) - 1]$ has the eigenvalue 0 for the eigenvector $(\{\dot{u}_i(0)\}, \{\ddot{u}_i(0)\})$ and thus is not invertible (then use algorithm 2). However, when there is a periodic external force with period t_b , applied to the oscillators, for example, to the phase twist at the boundary of the system, the time translation invariance of the solutions is broken so that breather and multibreather solutions can be found with this method.

Algorithm 2: In the case without any external force, our initial approach³ has been to restrict the working space to time reversible loops $X = (\{u_i(0), \dot{u}_i(0) = 0\})$ and to look for the fixed points of the truncated operator $T_R(\{u_i(0)\}) = \{u_i(t_b)\}$. The restricted Newton method only involves the $N \times N$ submatrix A of $[L_b(X) - 1]$ concerning the position variables of the oscillators which is invertible when $C \neq 0$. However, because the accuracy of this method can be shown to be intrinsically limited to (10^{-6}) with the standard computer accuracy (which is often sufficient), this method is improved for approaching the computer accuracy (10^{-13}) (see also Ref. 6). Considering the trying solution $x = \{u_i(0)\}$ with $\dot{u}_i(0) = 0$, our improved Newton algorithm is $x' = x - (A^*A + C^*C)^{-1}(A^*, C^*)[T_b(x, 0) - (x, 0)]$ where the $N \times N$ matrices A and C are defined as subblocks of the $2N \times 2N$ matrices $[L_b(X) - 1] = \begin{pmatrix} A & B \\ C & D \end{pmatrix}$ and where (A^*, C^*) is an $N \times 2N$ matrix.

Algorithm 3: For finding non-time-reversible solutions, this method has to be modified once again. Since we know that the perturbation of the trying solution in the direction of the eigenvector associated with the zero eigenvalues of the operator $[L_b(X) - 1]$ just changes the time origin of the solution, this perturbation is useless but it turns out to be harmful for the convergence of the Newton process because it involves large variations of the solution. This perturbation is removed by using the singular value decomposition⁷ of the

matrix $[L_b(X) - 1] = PVQ$ where P and Q are $2N \times 2N$ orthogonal matrices and V is a $2N \times 2N$ diagonal matrix with diagonal elements v_ν which contains an almost zero element v_0 . This matrix V is inverted in the space complementary to the vector $|0\rangle$ associated with the diagonal element with the smallest value which yields the ‘pseudo’ inverse matrix \tilde{V}^{-1} with diagonal elements $1/v_\nu$ for $\nu \neq 0$ and 0 for $\nu = 0$. Then, the Newton algorithm becomes $\{X' = X - Q^*\tilde{V}^{-1}P^*[T_b(X) - X]\}$.

When $C=0$, the matrix $[L_b(X) - 1]$ associated with a multibreather solution with p breathers, have p zero eigenvalues because of the breather phase degeneracy so that algorithm III does not converge in principle for C very small (except for the single breather state $p=1$). In practice, we calculate first a linearly stable time reversible multibreather solution with algorithm II up to some finite value of C for a 1D or 2D system with periodic boundary conditions. Then we make two identical boundary edges (or lines) by cutting the system along a line of oscillators where the motion of the oscillators is $u_i(t) = g_i(\omega_b t)$. Subsequently, we force a phase shift between the two edges of the system by forcing the motion to be $u_i^L(t) = g_i(\omega_b t - \alpha/2)$ on the left boundary and $u_i^R(t) = g_i(\omega_b t + \alpha/2)$ on the right boundary where α is a given phase. Then, algorithm I is used for relaxing the multibreather solution to an exact dynamical solution of the system under this boundary constraint. The phase α is incremented by small steps for having a continuous phase twist of the initial multibreather solution. When $\alpha = 2n\pi$ with n integer, the two boundaries of the system can be identified again. We use, subsequently, algorithm III (or variations with technical refinements) for relaxing the multibreather solution to an exact time periodic solution with period t_b of the system without constraint. The linear stability of the obtained solution is checked with a standard Floquet analysis.⁵

When the phase differences between the breathers are not multiples of π , the obtained solutions are not time reversible. The average energy flux on one period t_b through the bond between nearest-neighboring sites $\langle i, j \rangle$ is generally nonzero. It is the average work of the force of oscillator i onto oscillator j

$$J_{i \rightarrow j} = -J_{j \rightarrow i} = \frac{C}{t_b} \int_0^{t_b} u_i(t) \dot{u}_j(t) dt. \quad (4)$$

The first and simplest example we consider is a 1D chain with a breather at each site. The multibreather state with phase torsion $\alpha = qN$ makes a propagating anharmonic plane wave with wave vector $q = 2\pi n/N$. The energy flux through the bonds is conserved along the chain and depends on the wave vector q of this ‘anharmonic phonon’ (its frequency does not lie in the phonon band). Figure 1 shows two examples of variation of this energy flux for such multibreather states for the Morse potential and for the quartic potential.

This plane wave solution is not linearly stable in the whole interval of a phase torsion but only in an interval centered on π in the Morse case or centered on 0 in the quartic case.

One can also consider in the same way any other nonuniform distribution of breathers. Figure 2 shows two examples of multibreather solutions for the Morse and for the quartic

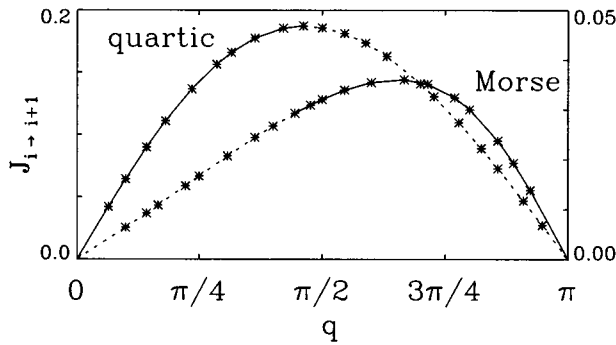


FIG. 1. Energy flux for the large amplitude anharmonic plane wave vs its wave vector in the 1D model for the quartic potential $C=0.1$, $\omega_b=1.7$, and for the Morse potential $C=0.1$, $\omega_b=0.8$ (energy scale magnified by 4). The full lines correspond to linearly stable anharmonic waves and the dotted line to linearly unstable ones.

potential which correspond to a uniform distribution of breathers (i.e., excited oscillators) except for a single breather vacancy. For all the figures, the sites with a breather (motion with a large amplitude) are represented by full dots and the vacancy(ies) by open dot(s). According to Ref. 5, the phase α_i of each oscillator i is defined as the average angle $\alpha_i = 1/t_b \int_0^{t_b} [\theta_i(t) - \omega_b t] dt$ over one period t_b of the motion in the standard action-angle representation $I_i(t), \theta_i(t)$. There is a large phase jump when crossing the bonds adjacent to the breather vacancy while the phase torsion between neighboring breathers is much weaker. The maximum energy flow which can be carried by the structure is much smaller because the breather vacancy acts as a strangle neck limiting the maximum energy flux.

For two-dimensional multibreather states, the global phase rigidity of multibreather structures can be stiffer provided the breathers arrange as a percolating cluster. Figure 3 shows a pattern of energy fluxes obtained with a single breather vacancy in the case of the Morse potential.

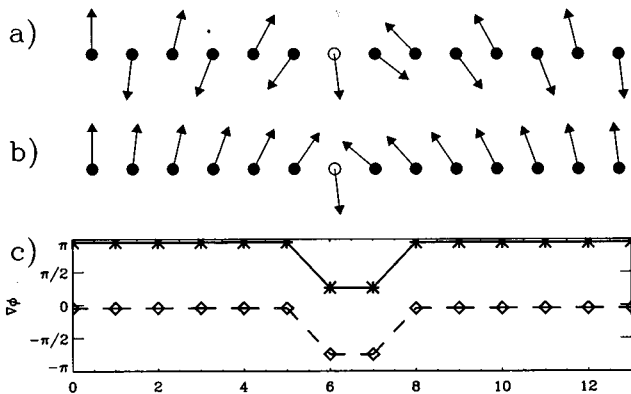


FIG. 2. Phase α_i vs i for a stable inhomogeneous wave obtained in 1D by phase torsion at the boundary as in Fig. 1 but for a multibreather state with a single breather vacancy for the Morse potential (a) at $\omega_b=0.8$, $C=0.04$, and for the quartic potential (b) at $\omega_b=1.8$, $C=0.25$. The orientation angle of the arrow is α_i . The phase gradient (wave vector) $q_i = \alpha_{i+1} - \alpha_i$ vs i (c) is almost constant and equal to π or 0 . It mostly varies in the vicinity of the breather vacancy.

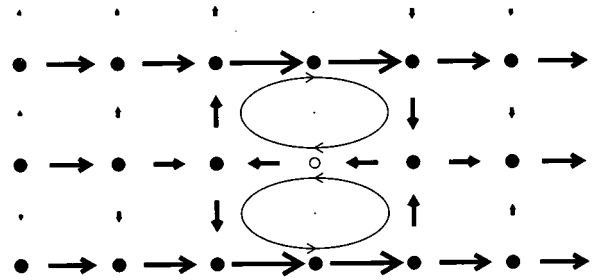


FIG. 3. Local distribution of the energy fluxes for a stable inhomogeneous wave obtained around a single breather vacancy calculated as for Fig. 2 but in a 2D system (size 15×4 , Morse potential at $C=0.02$ and $\omega_b=0.8$). The length of each arrow is proportional to the corresponding flux.

The energy flux is just distorted close to the breather vacancy which generates two symmetric vortex loops. By forcing nonuniform constraints at the boundary of the system, one can construct, in the same way, arbitrary connected multibreather states which also carry an energy flow. Figure 4 shows the pattern of the energy flux of a linearly stable solution which looks like a flowing “river” with meanders and a dead end. It is obtained from a percolating cluster of breathers connecting the two boundaries chosen at whim and submitted to a phase torsion.

One can also construct in 2D models⁵ finite clusters of breathers with just a single vortex in the energy flow. We choose first a solution at $C=0$ consisting of a cluster of breathers \mathcal{L} which form either a connected loop or more generally a disc with or without vacancies in the middle.

For C small, this continued configuration is linearly stable when the nearest-neighboring breathers are in phase for the hard quartic potential or in antiphase for the soft Morse potential. Next, we construct a trying solution by rotating the phases of the oscillators $i \in \mathcal{L}$ in an approximately uniform way in order to form a phase vortex. Then method III can be used and generally converges for C not too large. It yields an exact linearly stable multibreather solution which depends continuously on C with a vortex in the energy flow. In addition, the obtained solutions are spatially exponentially localized. Figure 5 shows such examples of vortices. With the

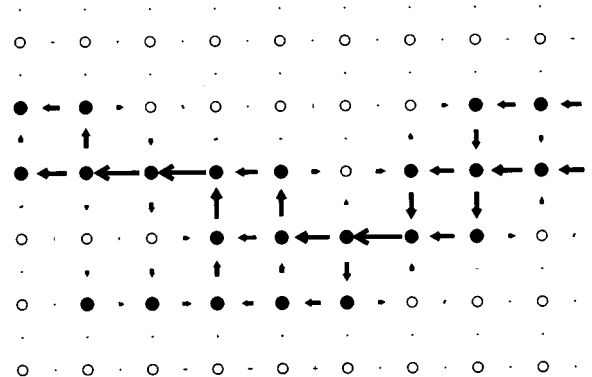


FIG. 4. Same as Fig. 3 but the initial breather distribution (black dots) has been chosen arbitrarily (quartic potential at $C=0.1$, $\omega_b=1.8$).

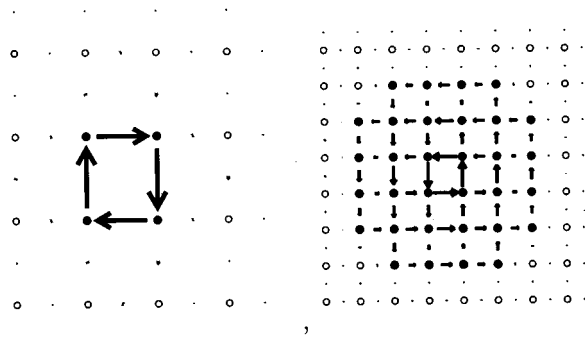


FIG. 5. A small and a big 2π vortex in the energy fluxes for the quartic potential at $C=0.1$, $\omega_b=1.7$.

same basic method, it is easy to construct at will a wide variety of more complex multibreather structures combining vortices and (or) antivortices, etc.

These multibreathers (with or without phase torsion) can survive as linearly stable structures for large coupling C in the hard quartic model provided their frequency ω_b is also chosen large. By contrast, for the soft Morse potential, these

structures are more fragile and only exist at rather small coupling C . In all cases, when the coupling C increases, they become linearly unstable much before anharmonics of their frequency ω_b enters the phonon band. These instabilities, which appear to be driven by phase fluctuations, have not been studied yet in detail. In addition, the multibreather structures can exist only when the single breather (the “bricks”) is well pinned to the lattice.⁶ When the breather depinning occurs, most corresponding multibreather structures are expected to collapse (pruning).

In summary, we have demonstrated that in strongly anharmonic systems, there may exist exact and stable solutions which can be viewed as highly distorted plane waves. Can these solutions form spontaneously? We suggest that we could get similar inhomogeneous patterns for the energy flow when forcing the penetration of energy through such an anharmonic system by a strong time periodic force with frequency ω_b at one edge of the sample. (Note that within a harmonic approximation, the incident wave should be reflected at that frequency.)

One of us (T.C.) acknowledges Conseil général de la région Rhône-Alpes for the grant Emergence and Laboratoire Léon Brillouin for its hospitality.

*Electronic address: tcretegn@physique.ens-lyon.fr

†Electronic address: aubry@bali.saclay.cea.fr

¹A. J. Sievers and S. Takeno, Phys. Rev. Lett. **61**, 970 (1988). See also S. Flach and C. Willis, Phys. Rep. (to be published).

²D. K. Campbell and M. Peyrard, in *CHAOS - Soviet American Perspectives on Nonlinear Sciences*, edited by D. K. Campbell (American Institute of Physics, New York, 1990).

³R. S. MacKay and S. Aubry, Nonlinearity **7**, 1623 (1994).

⁴J. L. Marín and S. Aubry, Nonlinearity **9**, 1501 (1996).

⁵S. Aubry, Physica D **103**, 201 (1997).

⁶Ding Chen, S. Aubry, and G. P. Tsironis, Phys. Rev. Lett. **77**, 4776 (1996).

⁷William H. Press *Numerical Recipes, the Art of Scientific Computing* (Cambridge University Press, Cambridge, England, 1986).